https://ntrs.nasa.gov/search.jsp?R=19800021439 2020-03-21T17:32:04+00:00Z

N O T I C E

THIS DOCUMENT HAS BEEN REPRODUCED FROM MICROFICHE. ALTHOUGH IT IS RECOGNIZED THAT CERTAIN PORTIONS ARE ILLEGIBLE, IT IS BEING RELEASED IN THE INTEREST OF MAKING AVAILABLE AS MUCH INFORMATION AS POSSIBLE

(NASA-CR-163429) THE RELATIONSHIPS BETWEEN HIGH LATITUDE CONVECTION REVERSALS AND THE ENERGETIC PARTICLE MORPHOLOGY OBSERVED BY THE ATMOSPHERE EXPLORER (Texas Univ. at Dallas, Richardson.) 33 p HC A03/MF A01 N80-29940

G3/46 Unclas 27434

THE RELATIONSHIPS BETWEEN HIGH LATITUDE CONVECTION REVERSALS AND THE ENERGETIC PARTICLE MORPHOLOGY OBSERVED BY ATMOSPHERE EXPLORER

R. A. Heelis, J. D. Winningham and W. B. Hanson
Center for Space Sciences
The University of Texas at Dallas
Richardson, TX 75080

J. L. Burch
Southwest Research Institute
San Antonio, TX 78284

Division of Earth & Physical Sciences
The University of Texas at San Antonio
San Antonio, Texas 78725

Abstract

Simultaneous measurements of the auroral zone particle precipitation and the ion convection velocity by Atmosphere Explorer show a consistent difference between the location of the poleward boundary of the auroral particle precipitation and the ion convection reversal. The difference, of about 1.5° of invariant latitude, is such that some part of the antisunward convection lies wholly within the auroral particle precipitation region. The nature of the convection reversals within the precipitation region suggests that in this region the convection electric field is generated on closed field lines that connect in the magnetosphere to the low latitude boundary layer.

Introduction

One of the outstanding problems of auroral physics still facing us after more than two decades of satellite based research is that of the fundamental, simultaneous, morphological relationships between low altitude convection (electric field), currents, and particle fluxes ($\lesssim$ 100 keV). Past missions have yet to successfully include all of the requisite instruments.

A confusion that this instrumental deficit generates is in the precise meaning of the term "polar cap," although it is generally accepted that the polar cap includes that region whose magnetic field maps into the distant magnetotail lobe. At present the term polar cap is used (and defined) when describing auroral particle precipitation, currents, convection, and optical data both individually and in combination. Various physical conclusions have been derived from using these definitions based on partial data sets and several contradictions have arisen. Chief among these is the determination of the "last closed field line" and the morphology of plasma, fields, and currents observed relative to this boundary.

The existence of a two cell convection pattern at high latitudes has been consistently confirmed by in-situ measurements of the ionospheric electric field made on rockets and satellites (Stern, 1977). Such a convection pattern leads quite naturally to the definition of a boundary near dawn and dusk that separates plasma flow at the highest latitudes, which has a component away from the sun, from flow at lower latitudes with a component toward the sun. This boundary, which has been called "the polar cap boundary," (and last closed field line, Gurnett and Frank, 1973) can be quite difficult to define near noon and midnight since the dominant components of the plasma flow there are not necessarily in the east-west direction (Heppner, 1972). It should also be noted that the two cell convection pattern may exist in a magnetospheric field topology that is completely closed (Axford and Hines, 1961) as well as one that is open (Dungey, 1961). Thus

the polar cap boundary defined by electric field or plasma convection measurements alone cannot be used to uniquely denote a boundary between open and closed field lines.

Frank and Gurnett (1971) and Gurnett and Frank (1973) used simultaneous plasma, energetic particle, and electric field data to investigate the relationships between the convection electric field, the energetic particle morphology, and the open or closed nature of the magnetic field. They concluded that near the dayside cusp the 45 keV electron trapping boundary, the gross convection electric field reversal, and the cusp equatorward boundary were colocated. They inferred further that on the dayside the electric field reversal marked the boundary between open and closed magnetic field lines. On the nightside, however, it was evident that the convection reversal usually lay within the "inverted V" precipitation regions, sometimes poleward and sometimes equatorward of the electron trapping region.

More recent data indicate that the conclusions mentioned in the previous paragraph may not be correct. Kintner et al. (1978) have shown that the equatorward boundary of the cusp identified by 180 eV electron precipitation is not coincident with the convection electric field reversal and is therefore not a good indicator of the open and closed field line boundary. Similar conclusions were reached by Heelis et al. (1976). In fact McDiarmid et al. (1976) have already shown on the basis of concurrent plasma and energetic particle data that the cusp is largely on closed field lines. In a later paper McDiarmid et al. (1979) employed concurrent energetic particle, plasma, and magnetic perturbation data to deduce a new "polar cap boundary" based on the maximum magnetic perturbation in the cleft. Such a definition when combined with the particle data placed most of the cleft region (McDiarmid et al., 1976) on closed field lines.

In a recent paper (McDiarmid et al., 1978) concurrent energetic electron, auroral electron, and magnetic field observations have been reported for the first time. In this paper the plasma convection direction was obtained from perturbations of the magnetic field relative to a model field. Using this method a comparison of >20 keV electrons and auroral electrons, with the concurrently observed magnetic perturbations, led McDiarmid et al. to conclude that in the region studied (0300 to 0900 and 1500 to 2100 MLT) (1) the reversal of convection from antisunward to sunward occurred within the poleward portion of the low altitude plasma sheet but not at its poleward boundary, (2) the plasma sheet is on closed field lines during these periods, thus placing the gross convection (electric field) reversal boundary on closed field lines, and (3) the poleward portion of the low-altitude plasma sheet connects along magnetic field lines to the magnetospheric boundary layer. The conclusions of McDiarmid et al. (1978) are in direct contradiction to the earlier mentioned Gurnett and Frank (1973) hypothesis, which used the electric field reversal as the indicator of the first open/closed field line boundary. The earlier criterion of Gurnett and Frank leads one to place, at times, a large fraction of the low-altitude extension of the plasma sheet on open field lines. Thus at present no consistent picture has emerged on what constitutes "the polar cap."

As an aid to distinguishing boundaries and features in the energetic particle precipitation at high latitudes, Winningham et al. (1975) coined the terms BPS (Boundary Plasma Sheet) and CPS (Central Plasma Sheet) to describe the temporal and spatial morphology of low altitude auroral electrons. The CPS was identified as a region of relatively uniform morphology as observed in an energy-time spectrogram. The spectra in this region are a combination of a Maxwellian plus power low spectrum (Deehr et al., 1976, Winningham et al., 1978, and Meng et al., 1978). In comparison the BPS is a region in which latitudinally structured precipitation is observed (Winningham et al., 1975, Figure 3a; Deehr et al.,

1976; and Meng et al., 1978) and in which substorm arcs occur (Deehr et al., 1976; Lui et al., 1977; and Winningham, et al., 1978). Electron spectra within the BPS exhibit a wide range of forms and their exact nature depends on their position relative to an auroral surge (Meng et al., 1978).

Based on the criterion for the BPS and CPS given by Winningham et al., (1975) and elaborated upon by Meng et al. (1978), the field line tilt reversal of McDiarmid et al. (1978) occurs in the BPS when their auroral electron flux profiles are examined. Thus their conclusions translate to the BPS being connected to the magnetospheric boundary layer, the BPS and CPS being on closed field lines, and the gross convection reversal occurring within the BPS during the times they studied.

In the present paper we will present results from the AE-C and -D energetic particle and thermal ion velocity instruments. Four boundaries will be scaled; the CPS equatorial edge, the CPS/BPS boundary, the BPS poleward edge, and the gross convection reversal. The definitions used earlier by Winningham et al., (1975) and reiterated in a previous paragraph will be used for scaling the particle data and the definitions of shear and rotational reversals given by Heelis and Hanson (1979) will be used for scaling the drift data.

The auroral particle results will be used as a bridge to other data sets that contain energetic particles, magnetic field, and optical results. An attempt will be made, with arguments of similarity to other data sets, to determine the region and field line topology in which the plasma convection reverses from anti-sunward to sunward. Comparison will be made to results in the equatorial plane and conclusions drawn as to the topological relationship between low and high altitude convection and the "openness" or "closedness" of the portion of the magnetosphere most relevant to low altitude auroral zone phenomena.

Instrumentation

The data used in this study were taken from AE-C and AE-D. The AE-C spacecraft was launched in December, 1973 into a 68° inclination orbit with initial nominal apogee and perigee of 4000 km and 150 km, respectively. After about 1 year of operation in an elliptical orbit, the orbit was circularized and the satellite operated at various altitudes between 280 km and 450 km. The AE-D spacecraft was launched in October 1975 into a 90° inclination orbit with the same initial apogee and perigee as AE-C and operated in this orbit until its demise in February 1976. Both satellites were utilized for roughly equal numbers of orbits in a spinning (4 rpm) and a despun (1 revolution per orbit) mode. Data used in this study were obtained when the spacecraft were despun. The ion convection velocity is obtained from the RPA and the Drift Meter and has an overall accuracy of $\pm 10\%$ or ± 40 m s^{-1}, whichever is larger. Details of the instrument and techniques involved are given by Hanson et al. (1973) and Hanson and Heelis (1975). The energetic particle spectra are obtained from the low energy electron experiment (LEE) which measured the differential flux of electrons in 16 contiguous energy channels covering the range 200 eV to 25 keV (Hoffman et al., 1973). On AE-C two analyzers, one for electrons and one for ions, were used to step through the entire spectrum and another was used for fixed energy electrons. On AE-D, three analyzers were used for stepping and 16 were operated at fixed energy. Details of the AE spacecraft and full instrumentation appear in the April 1973 issue of Radio Science.

Observations

We report here the results from 87 crossings of the nightside auroral zone by Atmosphere Explorers C and D. The data were restricted to times when the convection reversal boundary could be unambiguously located from ion drift velocity measurements and at the same time the auroral particle detector was sampling a component of the primary spectrum. The auroral particle spectrograms of differential energy flux versus energy and time were used to locate the equatorial edge of >200 eV particle precipitation, the poleward edge of the auroral precipitation and the boundary between the boundary plasma sheet precipitation and the central plasma sheet precipitation. Figure 1 shows the energetic particle spectrogram for a pass of AE-C across the nightside high latitude ionosphere in the southern hemisphere. The equatorwardmost precipitation region shows a uniform total energy flux and spectral shape with a mean energy between 1 and 5 keV from about 19:10 UT to 19:11 UT. Examination of the detailed spectral data indicates that the spectra in this region are comprised of a lower energy ($\lesssim$ 1 to 2 keV) power law portion plus a higher energy section that is relatively flat for a range of energies ($\sim$ 1 to 10 keV) and then precipitiously drops in flux. Such spectra are consistent with the definition of the CPS given earlier. The CPS is distinguished from the BPS by the onset of peaked spectra (inverted V's) and a much more structured and larger total energy input that may vary from 0.1 to 3 ergs/cm^2 ster sec (i.e. greater spatial/temporal structure) in the region between 19:11 UT and 19:12:30 UT. The disappearance of precipitation at energies above 1 keV quite precisely defines the boundary between the poleward edge of the auroral zone and the polar rain. The abrupt disappearance of proton precipitation at this boundary may also be seen.

On the morning side the CPS has a much higher mean energy but is again quite separable from the BPS due to the difference in spectral type. The shaded area indicates the degree of uncertainty in determination of the CPS/BPS boundary. Figure 2 shows the two components of the horizontal ion velocity measured simultaneously with the data shown in Figure 1. V_x along the satellite track and V_z perpendicular to the satellite track are plotted as a function of time for comparison with Figure 1 and on an invariant latitude magnetic local time dial to more clearly illustrate the nature of the convective flow. Here a visible description of the convection reversals separating sunward from anti-sunward flow agrees easily with the quantitative classification given by Heelis and Hanson (1979). Both reversals can be quite precisely located at 19:11:50 and 19:19:20 UT and may be called "shear" in nature since there is only a very small component of flow (V_x) across the reversal. In both cases it can be seen that the poleward particle boundary lies poleward of the convection reversal. The format of the AE spectrograms is identical and directly comparable to that used by Winningham et al. (1975) to originally define the BPS and CPS. The detailed spectral characteristics that distinguish the BPS and CPS have been given by Winningham et al. (1975), Deehr et al. (1976) and Meng et al. (1978) and were repeated earlier. While this leads to some uncertainty in the location of the boundary between the CPS and the BPS it does not invalidate the finding that the poleward edge of the BPS lies poleward of the shear convection reversal. These displacements are easily resolvable, being about 40 sec (≈300 km) on the evening side and about 60 sec (≈500 km) on the morning side. It should also be noted that in this case, where shear reversals define the convection boundary, the reversals are embedded in the BPS precipitation

region. Thus the BPS occupies a region where the plasma in the ionosphere is moving both sunward and antisunward.

In addition to shear reversals separating sunward and antisunward convection near dawn and dusk, the high latitude ionospheric convection pattern shows evidence for well defined rotational reversals as the antisunward flow at high latitudes moves toward lower latitudes near midnight. Figures 3 and 4 are typical of the observed relationships between the particle precipitation regions and the convection reversal in such cases. Here we focus attention on the rotational reversal that is quite clearly seen near 22:00 hrs MLT and 67° invariant latitude in Figure 4. This figure shows that the reversal is characterized by at least 1 minute (≈450 km) along the satellite track at 20:39 UT where the larger component of ion velocity V_x is across the reversal boundary. Again the equatorward and poleward edges of the particle precipitation zone can quite easily be seen in the auroral particle spectrogram. The boundary between the CPS and the BPS is observed at ∿20:40:45 UT as a change to peaked inverted V spectra. Reference to Figure 4 demonstrates that the CPS/BPS boundary lies at or across the rotational convection reversal.

The fact that the BPS may lie wholly on antisunward convecting field tubes associated with rotational flow is demonstrated further in Figure 5. This figure shows two rotational reversals at magnetic local times of about 22:00 hrs and 02:30 hrs. These reversals mark the boundary between antisunward and sunward flow and also the boundary between BPS and CPS particle precipitation. In this case the entire region of antisunward flow coincides with the region of BPS precipitation. Observations of this kind must imply that as we move along the meridian from midnight toward noon we must at some place encounter the boundary between the BPS and the polar rain (Winningham and Heikkila, 1974) in a region of antisunward convection.

Figure 6 shows such an observation. This pass of AE-D across the northern hemisphere shows again that the CPS/BPS boundary coincides approximately with the rotational reversal even near midnight. Again the BPS resides on a region

of antisunward convection and the boundary between the BPS and the polar rain shows no significant signature in the convection pattern.

Examination of 87 passes of Atmosphere Explorer in the high latitude ionosphere has been carried out to identify the convection reversal boundary and the boundaries of the particle precipitation zones described previously. We have examined this data both statistically and on a case by case basis. Statistically each boundary has been represented by a circle using a least squares technique to determine the center and the radius. The locations of the poleward edge of the particle precipitation zone, the CPS/BPS boundary, the equatorward edge of the precipitation zone and the ion convection velocity reversal are shown in Figure 7. Also shown by the solid lines are the best fit circles to these boundaries. The MLT and latitude of the center and the radius in degrees for each circle are shown in the top right of each figure. It can be seen that very little data from the dayside were included in this study and no attempt was made to limit the observations to a similar magnetic activity condition. The significance of these results lies in the statistical displacement of the convection reversal boundary with respect to the poleward edge of the particle precipitation zone. While we cannot attribute any physical significance to the position and size of the circles, it is worth noting that the centers and radii of the best fit circles for the CPS/BPS and convection reversal are very close to the values reported by Meng et al. (1977) for the quiet auroral belt circle. Figure 8 shows the relative positions of the CPS and BPS precipitation zones with respect to the convection reversal boundary. The CPS precipitation zone is seen (Figure 7) to increase in extent between midnight and 06:00 hrs MLT as one would expect in accordance with the gradient and curvature drift of particles in the equatorial plane. Near midnight the CPS/BPS boundary and convection reversal boundary are quite close

together in accordance with our findings that the rotational reversals tend to coincide with the CPS/BPS boundary. The displacement of the point of closest coincidence toward 21:00 hrs is most likely produced by the statistical domination of points in the 24:00 hrs to 06:00 hrs MLT sector. At other magnetic local times on the nightside the convection reversal lies within the BPS precipitation zone with the poleward edge of this zone typically lying about 2° poleward of the convection reversal.

On a case by case basis, passes that cut almost radially through the auroral zone have been considered. For each satellite pass the magnetic local times of the poleward and equatorial edge of the particle precipitation zone were recorded. Only passes where these local times differed by less than 2 hrs in the nighttime MLT sector between 18:00 hrs to 06:00 hrs were considered. In the most favorable longitude zone the AE-C satellite moves from 62° to 72° invariant latitude in approximately 1 hour of magnetic local time. For the selected passes the position of the convection reversal is plotted against the position of the poleward particle boundary and the CPS/BPS boundary in Figure 9. Here the solid lines show where the two boundaries would be coincident. Of the 32 cases considered only four show coincidence between the convection reversal and the poleward edge of the particle precipitation region. For all other cases the poleward particle boundary lies poleward of the convection reversal and the average displacement is about 1.5° of invariant latitude. It can also be seen that in general the convection reversal lies poleward of the CPS/BPS boundary. This indicates that the change from sunward to antisunward convection in the nightside ionosphere occurs within the BPS and in a region usually associated with closed field lines, i.e. the low altitude extension of the plasma sheet.

Discussion

It has been pointed out that the AE drift (electric field) measurements used here cannot distinguish between open and closed field line geometries, but we may appeal to previous studies of the location of trapped 40 keV electron boundary relative to the lower energy BPS precipitation region (McDiarmid et al., 1976) to conclude that the BPS is associated with field tubes that are closed. The results shown here indicate that the BPS precipitation region may be wholly or partially in a region associated with antisunward flow in the ionosphere. This confirms the earlier inferences of McDiarmid et al. (1978) and Winningham et al. (1978) based on indirect evidence. The relevance of these findings to the flow of plasma in the magnetotail depends on our ability to relate flow regimes in the ionosphere to corresponding regimes in the magnetosphere. The nature of the convection reversals which lie within the BPS may be an important factor in determining the location of different plasma regimes in the magnetotail. Figure 10 shows, schematically, corresponding particle and flow regions in the polar ionosphere and the magnetotail. We suggest that a shear reversal quite uniquely distinguishes flow that is sunward from flow that is antisunward, both in the ionosphere and in the equatorial plane of the magnetosphere. The region of shear reversals is thus placed at the flanks of the magnetotail. Since BPS particle precipitation is generally observed poleward and equatorward of the reversal, the reversal occurs within the equatorial boundary layer as shown. If some region of the antisunward flow poleward of a shear reversal results from a viscously driven convection pattern, it might be expected that the BPS precipitation would result from plasma interactions at the boundary of the solar wind and the magnetopause and at the boundary between the antisunward convecting viscous layer and the sunward convecting plasma sheet. In such a case the BPS would

span the convection reversal as observed (cf. Sonnerup, 1979). The observation of shear convection reversals that lie equatorward of the poleward BPS precipitation region as shown in Figures 1 and 2 is the most convincing evidence at low altitudes for antisunward flow in a boundary layer of the magnetotail.

At local times toward midnight we have shown that the more commonly observed rotational reversals are usually associated with the CPS/BPS boundary. The rotational reversal mapping into the equatorial plane is rather arbitrary and serves only to indicate its relationship to the particle precipitation regions. It is also true that the boundary between the CPS and BPS may not always be well defined. The point to note here is that a rotational reversal does not necessarily separate oppositely flowing plasma regions in the magnetosphere. In general, after the plasma has undergone a rotational reversal (and has by definition a sunward component in the ionosphere) it is observationally associated with CPS particle precipitation. In these cases we associate this flow regime with sunward flow on closed field lines in the plasma sheet. The CPS particle precipitation could result from simple betatron acceleration as the particles convect toward the earth and their mirror points move to lower altitudes.

In the midnight period dominated by rotational flow it should be noted that before undergoing a clear rotational reversal, the entire antisunward flowing plasma region in the ionosphere may be associated with BPS particle precipitation. It can be seen th this antisunward flowing region in the ionosphere is associated with sunward flowing plasma in the equatorial plane on highly distended, closed non-dipolar field lines. Corresponding points labelled A and B on the convective trajectories in the ionosphere and magnetosphere are shown to illustrate this behavior. It should be pointed out that with the conclusions drawn here, the point at which

the convection reversal ceases to be a shear, marks a corresponding point in the equatorial plane where the antisunward flow in the boundary layer begins to turn sunward. If we do not consider the existence of some widely distributed well ordered pattern of field aligned potential drops, which may lead to the different location of the convection reversal and the poleward BPS boundary, then we must conclude that at least some portion of the two cell convection pattern of both flow senses observed at high latitudes in the ionosphere, exists entirely on closed field lines. From the point of view of low altitude observations we may regard the magnetosphere as open or closed, depending on the geometry of the magnetic flux tubes that are convecting antisunward at high latitudes. Then, again, without the assumption about field aligned potentials, must conclude from this study that a "completely" open magnetosphere, i.e. a magnetosphere in which all antisunward convecting field tubes are open, does not exist. In the magnetotail we expect a plasma sheet cross section that has its flanks dragged further away from the earth than its center (Russell, 1977) and a convection electric field generated in the low latitude boundary layer (Eastman et al., 1976) by a viscous interaction between the solar wind and the magnetospheric plasma. We note Russell (1977) has pointed out that such a magnetotail cross section does not imply a completely closed magnetosphere. Our observations are consistent with either a completely closed magnetosphere or a partially open and partially closed magnetosphere, (Crooker, 1979), but not an open magnetosphere in which the last closed field line, the end of the plasma sheet, and the convection reversal are coincident.

It is customarily thought that the polar rain precipitation (Winningham and Heikkila, 1974) is associated with open field tubes attached to the interplanetary magnetic field. In such a configuration the cleft marks the region in which the connection of interplanetary magnetic field and geomagnetic field

takes place. Then the antisunward convection in the central polar cap corresponds to the antisunward convection in the solar wind with subsequent convection across a nightside neutral line near the equatorial plane in the magnetotail. Presumably this neutral line, which separates open field lines from closed field lines, lies at the poleward boundary of the BPS (and equatorward boundary of the polar rain) on the nightside of the polar cap as shown in Figure 10. The observations reported here show no readily observable ionospheric flow characteristics across this boundary. However, in the ionosphere the boundary between the BPS and the polar rain precipitation is very sharp and it is necessary to reconcile this difference in particle populations within different regions in the plasma sheet in order that a completely closed magnetosphere be acceptable. This is perhaps a more serious constraint on a closed model than the entry of solar flare particles discussed by Piddington (1979).

Conclusions

A statistical study and a case by case study of simultaneous particle and ion convection velocity measurements from Atmosphere Explorer show that at all local times between 18:00 hrs and 06:00 hrs the gross convection reversal boundary lies equatorward of the boundary between the discrete, highly structured BPS precipitation and the polar rain. This study reveals quite convincing evidence for the existence of shear and rotational convection reversals on closed field lines. The observed morphology is consistent with a partially closed magnetosphere in which some portion of the convection electric field is generated in the low latitude boundary layer. An open magnetosphere in which the last closed field line, the plasma sheet outer boundary, and the convection reversal are coincident is not immediately consistent with these findings.

Acknowledgments

We would like to thank Drs. W. J. Heikkila, E. W. Hones, Jr., and S.-I. Akasofu, for helpful discussions, and R. A. Power and S. A. Fields for computing efforts and preparation of spectrograms. We thank R. A. Hoffman for making available the low energy particle data. This work was supported by National Science Foundation Grant DES75-03985 and by National Aeronautics and Space Administration Grant NSG5085 and NASA Contract NAS5-11407.

REFERENCES

Axford, W. I. and C. O. Hines, A unifying theory of high latitude geophysical phenomena and geomagnetic storms, Can. J. Phys., 39, 1433, 1961

Crooker, N. U., Dayside merging and cusp geometry, J. Geophys. Res., 84, 951, 1979

Deehr, C. S., J. D. Winningham, F. Yasuhara, and S.-I. Akasofu, Simultaneous observations of discrete and diffuse auroras by the ISIS 2 satellite and airborne instruments, J. Geophys. Res., 81, 5527, 1976

Dungey, J. W., Interplanetary magnetic field and the auroral zones, Phys. Rev. Lett., 6, 47, 1961

Eastman, T. E., E. W. Hones. Jr., S. J. Bane and J. R. Asbridge, The magnetospheric boundary layer: Site of plasma, momentum and energy transfer from the magnetosheath into the magnetosphere, Geophys. Res. Lett., 3, 685, 1976

Frank, L. A. and D. A. Gurnett, Distributions of plasmas and electric fields over the auroral zones and polar caps, J. Geophys. Res., 76, 6829, 1971

Gurnett, D. A. and L. A. Frank, Observed relationships between electric fields and auroral particle precipitation, J. Geophys. Res., 78, 145, 1973

Hanson, W. B. and R. A. Heelis, Techniques for measuring bulk flow velocities from satellites, Space Sci. Instrum., 1, 493, 1975

Hanson, W. B., D. R. Zuccaro, C. R. Lippincott and S. Sanatani, The retarding potential analyzer on Atmosphere Explorer, Radio Sci., 8, 333, 1973

Heelis, R. A. and W. B. Hanson, High latitude ion convection in the nighttime F-region, submitted to J. Geophys. Res., 1979

Heelis, R. A., W. B. Hanson and J. L. Burch, Ion convection velocity reversals in the dayside cleft, J. Geophys. Res., 81, 3803, 1976

Heppner, J. P., Electric fields in the magnetosphere, Initial Problems of Magnetospheric Physics, ed. E. R. Dyer, p. 107, IUCSTP Secretariat, Washington, D. C., 1972

Hoffman, R. A., J. L. Burch, R. W. Janetzke, J. F. McChesney, S. H. Way and D. S. Evans, Low energy electron experiment for Atmosphere Explorers C and D, Radio Sci., 8, 393, 1973

Kintner, P. M., K. L. Ackerson, D. A. Gurnett and L. A. Frank, Correlated electric field and low energy electron measurements in the low altitude polar cusp, J. Geophys. Res., 83, 163, 1978

Lui, A. T. Y., D. Venkatesan, C. D. Anger, S.-I. Akasofu, W. J. Heikkila, J. D. Winningham, and J. R. Burrows, Simultaneous observations of particle precipitations and auroral emissions by the ISIS 2 satellite in the 19-24 MLT sector, J. Geophys. Res., 82, 2210, 1977

McDiarmid, I. B., J. R. Burrows, and E. E. Budzinski, Particle properties in the day side cleft, J. Geophys. Res., 81, 221, 1976

McDiarmid, I. B., J. R. Burrows, and M. D. Wilson, Comparison of magnetic field perturbations at high latitudes with charged particle and IMF measurements, J. Geophys. Res., 83, 681, 1978

McDiarmid, I. B., J. R. Burrows, and Margaret D. Wilson, Large-scale magnetic field perturbations and particle measurements at 1400 km on the dayside, J. Geophys. Res., 84, 1431, 1979

Meng, C.-I., R. H. Holzworth and S.-I. Akasofu, Auroral Circle - Delineating the poleward boundary of the Quiet Auroral Belt, J. Geophys. Res., 82, 164, 1977

Meng, C.-I., A. L. Synder, Jr., and H. W. Kroehl, Observations of auroral westward traveling surges and electron precipitations, J. Geophys. Res., 83, 575, 1978

Piddington, J. H., The closed model of the earth's magnetosphere, J. Geophys. Res., 84, 93, 1979

Russell, C. T., Some comments on the topology of the geomagnetic tail, J. Geophys. Res., 82, 1625, 1977

Stern, D. P., Large-scale electric fields in the earth's magnetosphere, Rev. Geophys. Space Phys., 15, 156, 1977

Sonnerup, Buö, Theory of the low latitude boundary layer, Proc. Magnetospheric Boundary Layers Conf., ESA-SP-148, 395, 1979

Winningham, J. D. and W. J. Heikkila, Polar cap auroral electron fluxes observed with ISIS I, J. Geophys. Res., 79, 1393, 1974

Winningham, J. D., F. Yasuhara, S.-I. Akasofu, and W. J. Heikkila, The latitudinal morphology of 10 eV to 10 KeV electron fluxes during magnetically quiet and disturbed times in the 21:00 to 03:00 MLT sector, J. Geophys. Res., 80, 3148, 1975

Winningham, J. D., C. D. Anger, G. G. Shepherd, E. J. Weber, and R. A. Wagner, A case study of the aurora, high-latitude ionosphere, and particle precipitation during near-steady state conditions, J. Geophys. Res., 83, 5717, 1978

Figure Captions

Figure 1. Energetic particle spectrogram for southern hemisphere pass of AE-C orbit 13064. The position of the BPS and CPS are shown and the shaded region denotes the degree of uncertainty in determining the CPS/BPS boundary.

Figure 2. Simultaneously measured horizontal ion convection velocity for AE-C orbit 13064 showing the existence of shear reversals marking the boundary between sunward and antisunward convection. The position of the CPS and BPS are shown on all panels.

Figure 3. Energetic particle spectrogram for southern hemisphere pass of AE-C orbit 11643.

Figure 4. Simultaneously measured horizontal ion convection velocity for AE-C orbit 13064 showing the existence of rotational reversals marking the boundary between sunward and antisunward convection. The position of the CPS and BPS are shown on all panels.

Figure 5. Observed morphology of the BPS and CPS near midnight showing the BPS entirely on antisunward convecting field tubes.

Figure 6. Simultaneous measurements from AE-D show the boundary between the BPS and the polar rain near midnight is on antisunward convecting field tubes.

Figure 7. Individual data points and least square fit circles denoting the particle and convection reversal boundaries. The position of the center and radius of each circle is shown in the top right.

Figure 8. Statistical placement of the convection reversal within the particle precipitation regions.

Figure 9. Results of a case by case study of the relative positions of the particle and convection boundaries. The solid line denotes the position of colocated boundaries.

Figure 10. Schematic configuration of ionospheric and magnetospheric particle and flow regions.

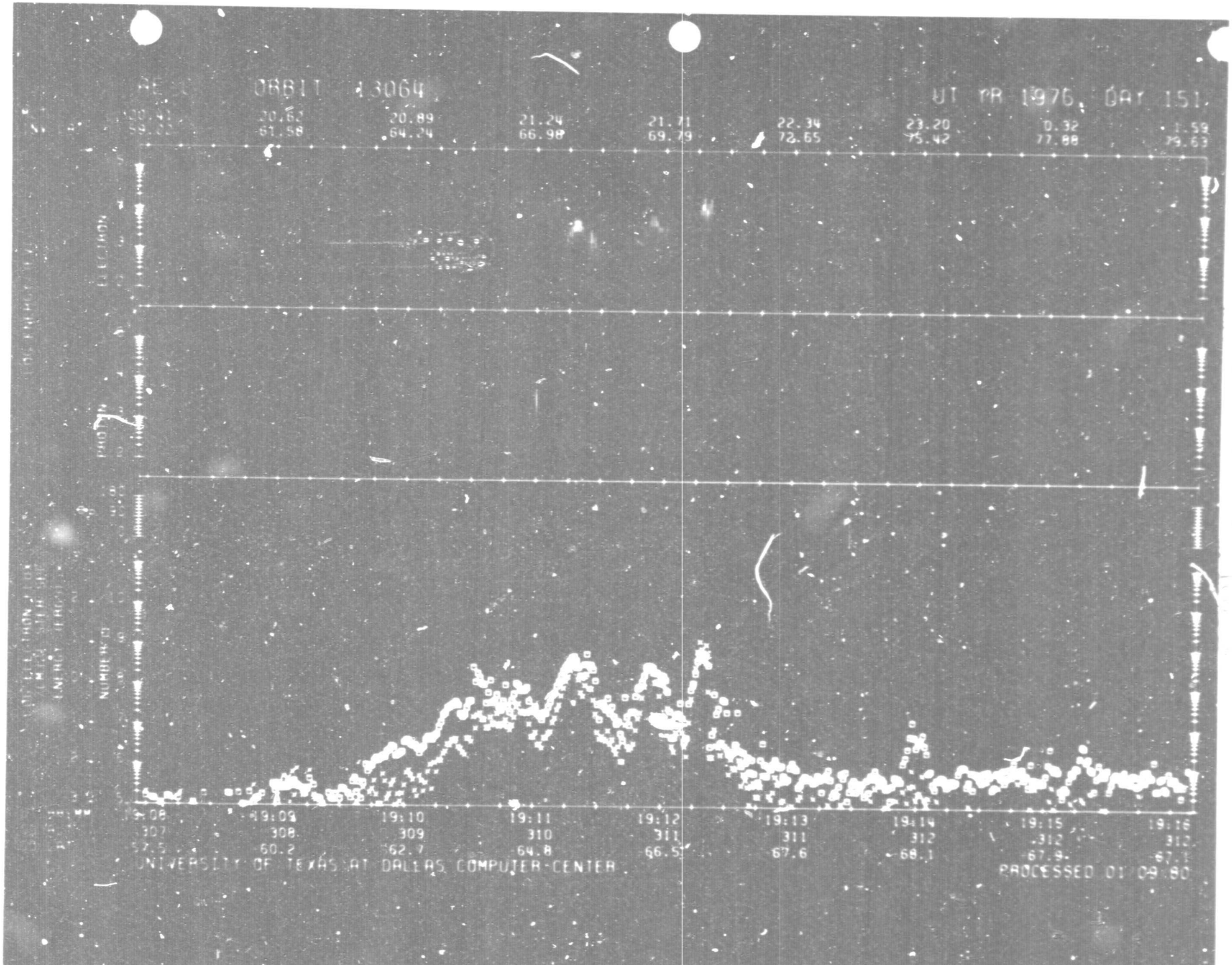
ORBIT 13064
UT YR 1976, DAY 151
20.62 20.89 21.24 21.71 22.34 23.20 0.32 1.59
61.58 64.24 66.98 69.79 72.65 75.42 77.88 79.63
ELECTRON
PROTON
NUMBER
19:08 19:09 19:10 19:11 19:12 19:13 19:14 19:15 19:16
307 308 309 310 311 311 312 312 312
57.5 60.2 62.7 64.8 66.5 67.6 68.1 67.9 67.1
UNIVERSITY OF TEXAS AT DALLAS COMPUTER CENTER
PROCESSED 01 09 80

ORIGINAL PAGE IS
OF POOR QUALITY

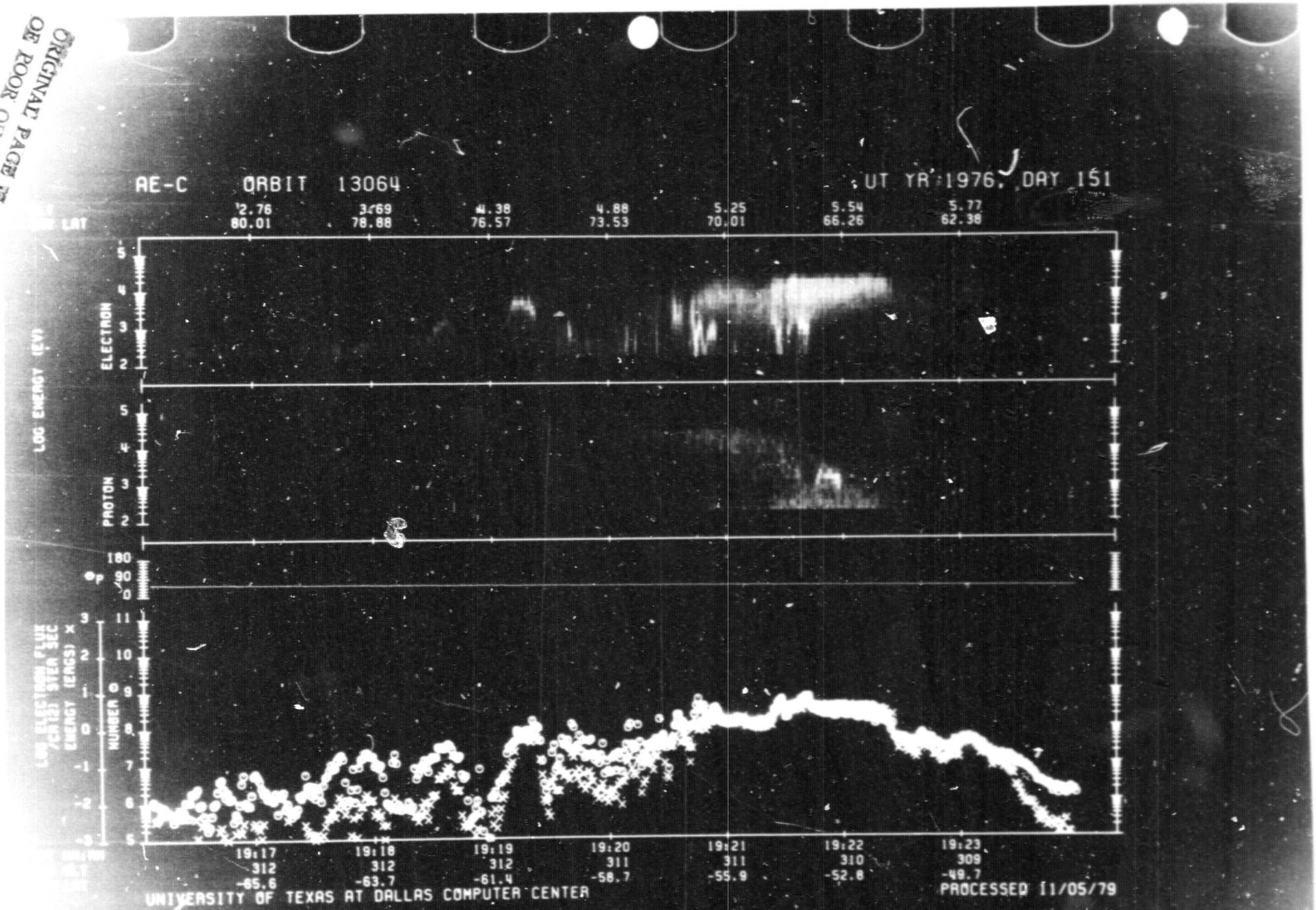

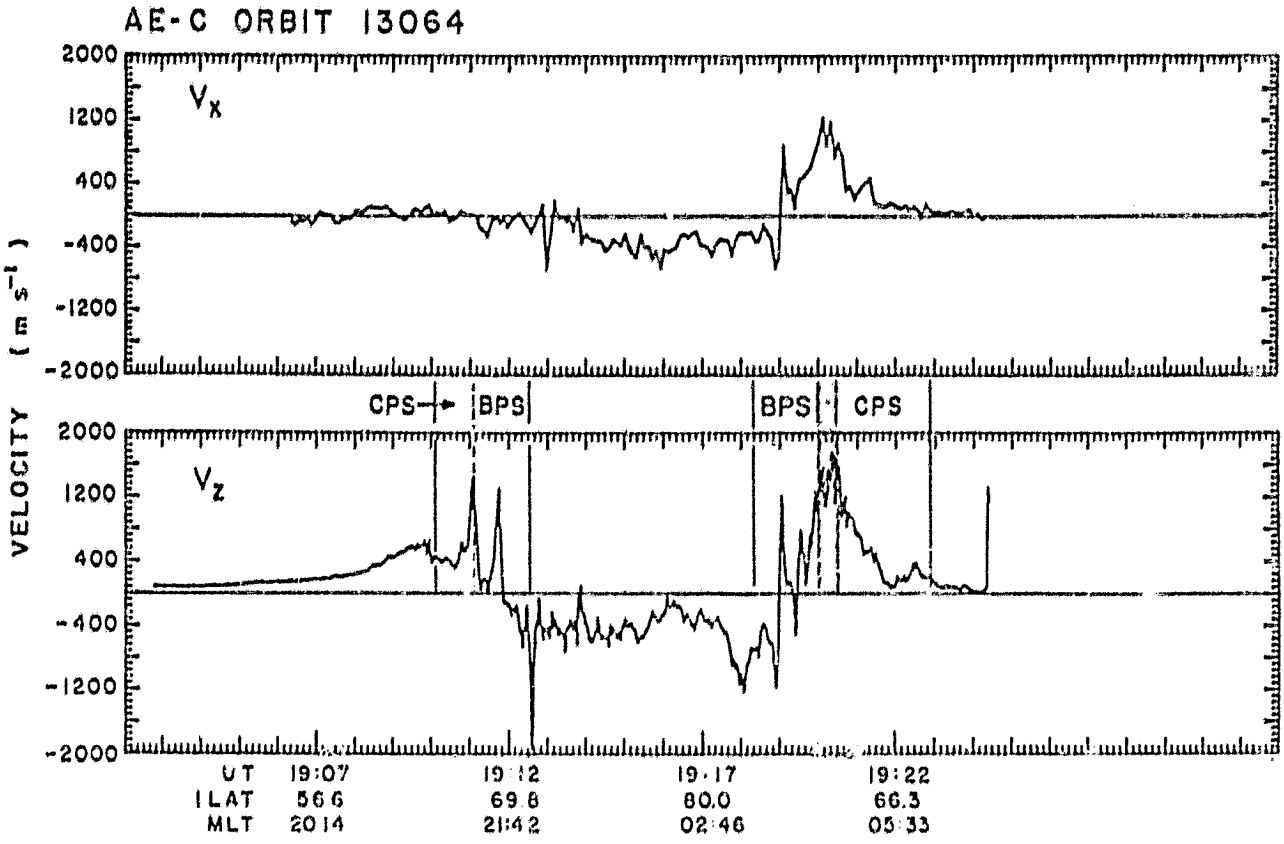

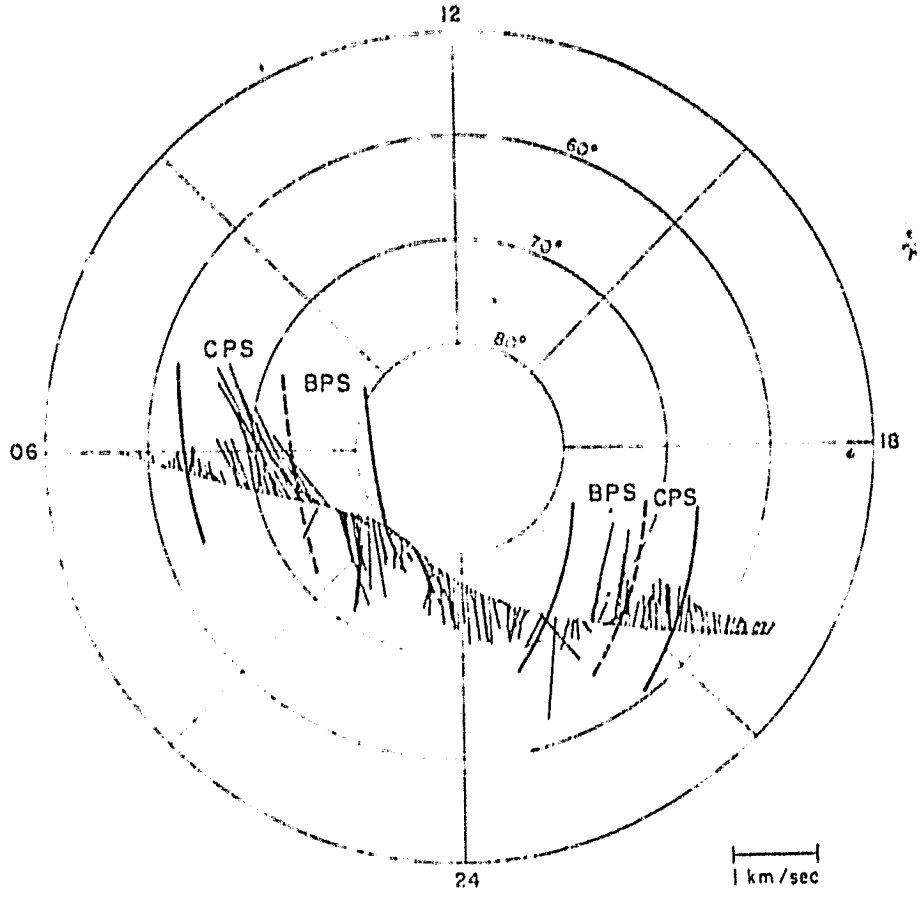

SOUTHERN HEMISPHERE
MLT vs INV LAT

FIGURE 2

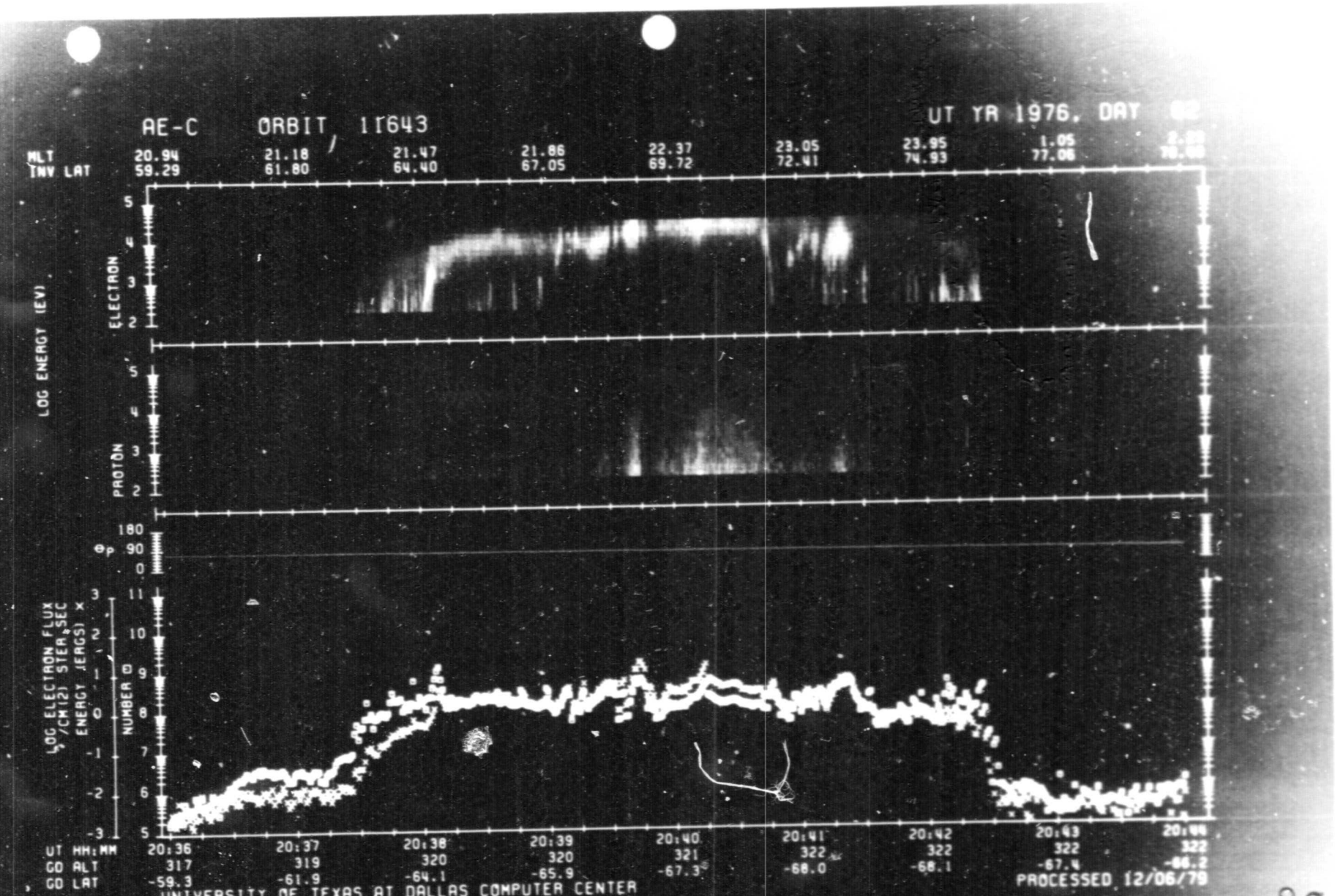

ORIGINAL PAGE IS
OF POOR QUALITY

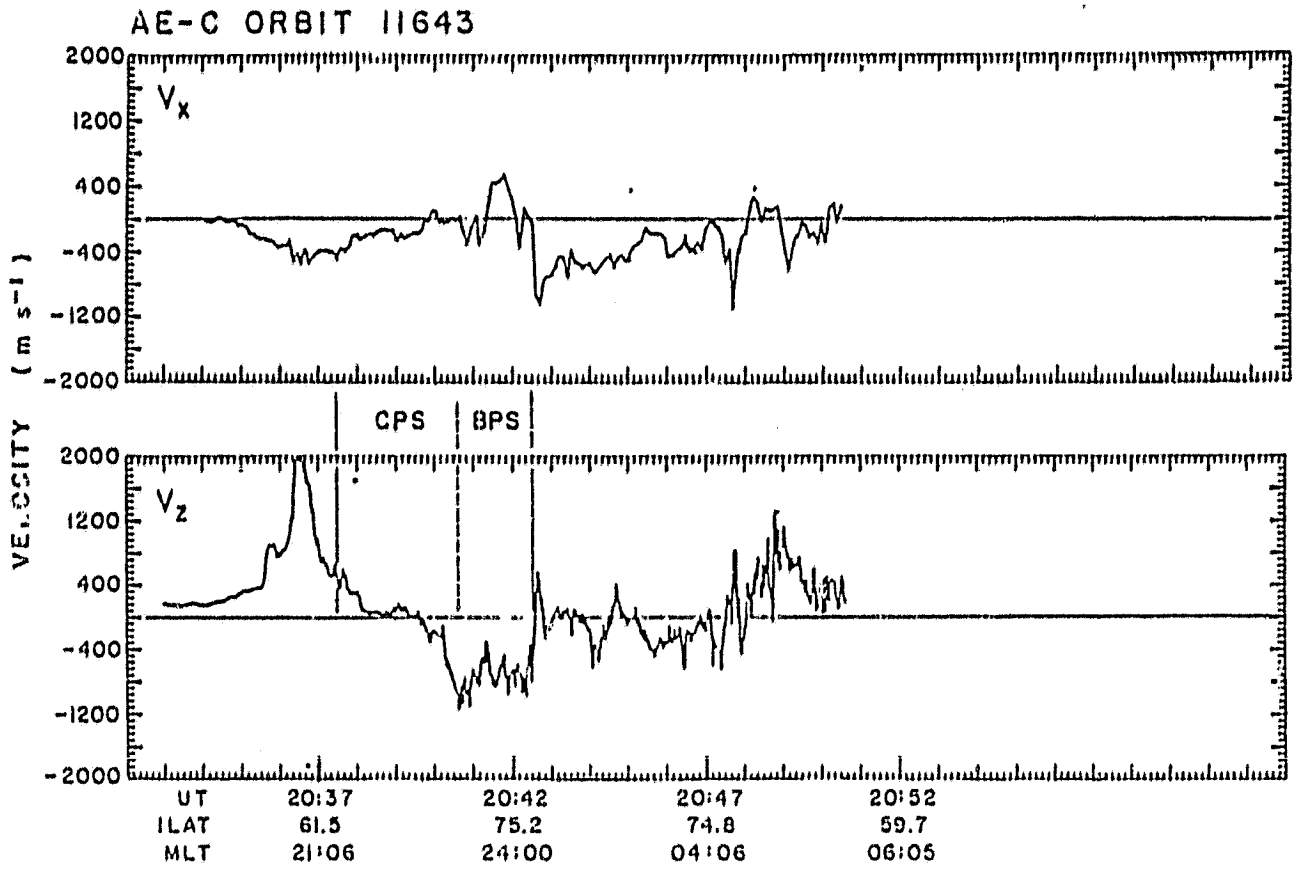

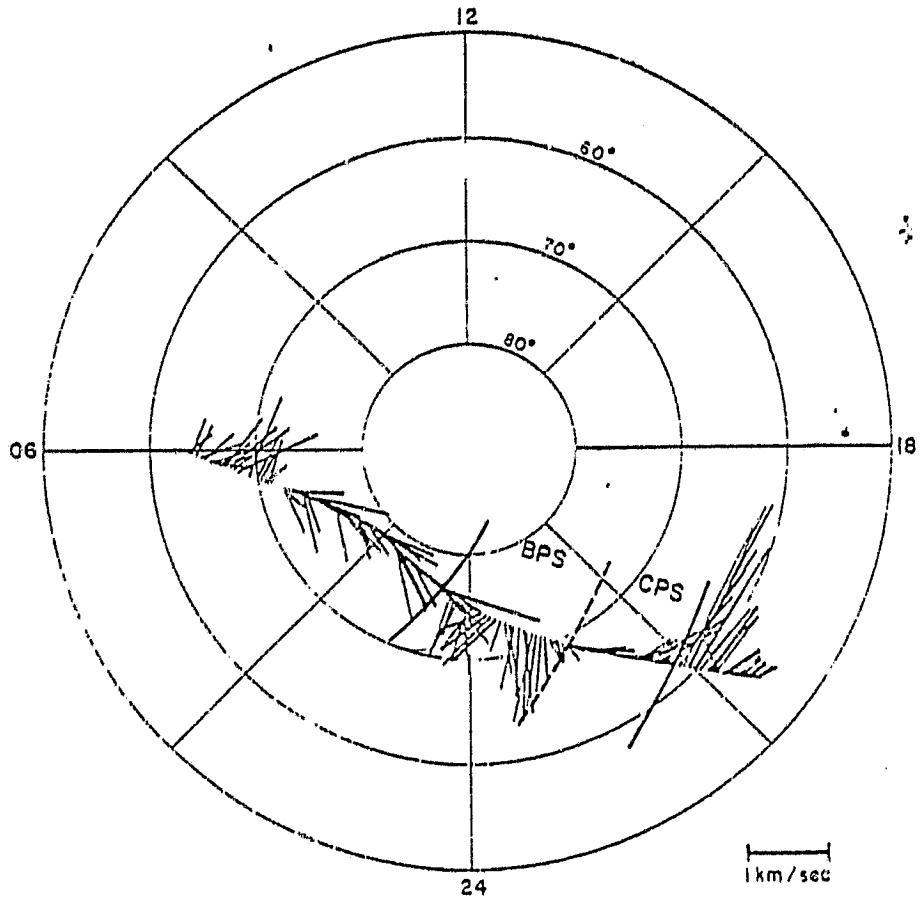

FIGURE 4 SOUTHERN HEMISPHERE
MLT vs INV LAT

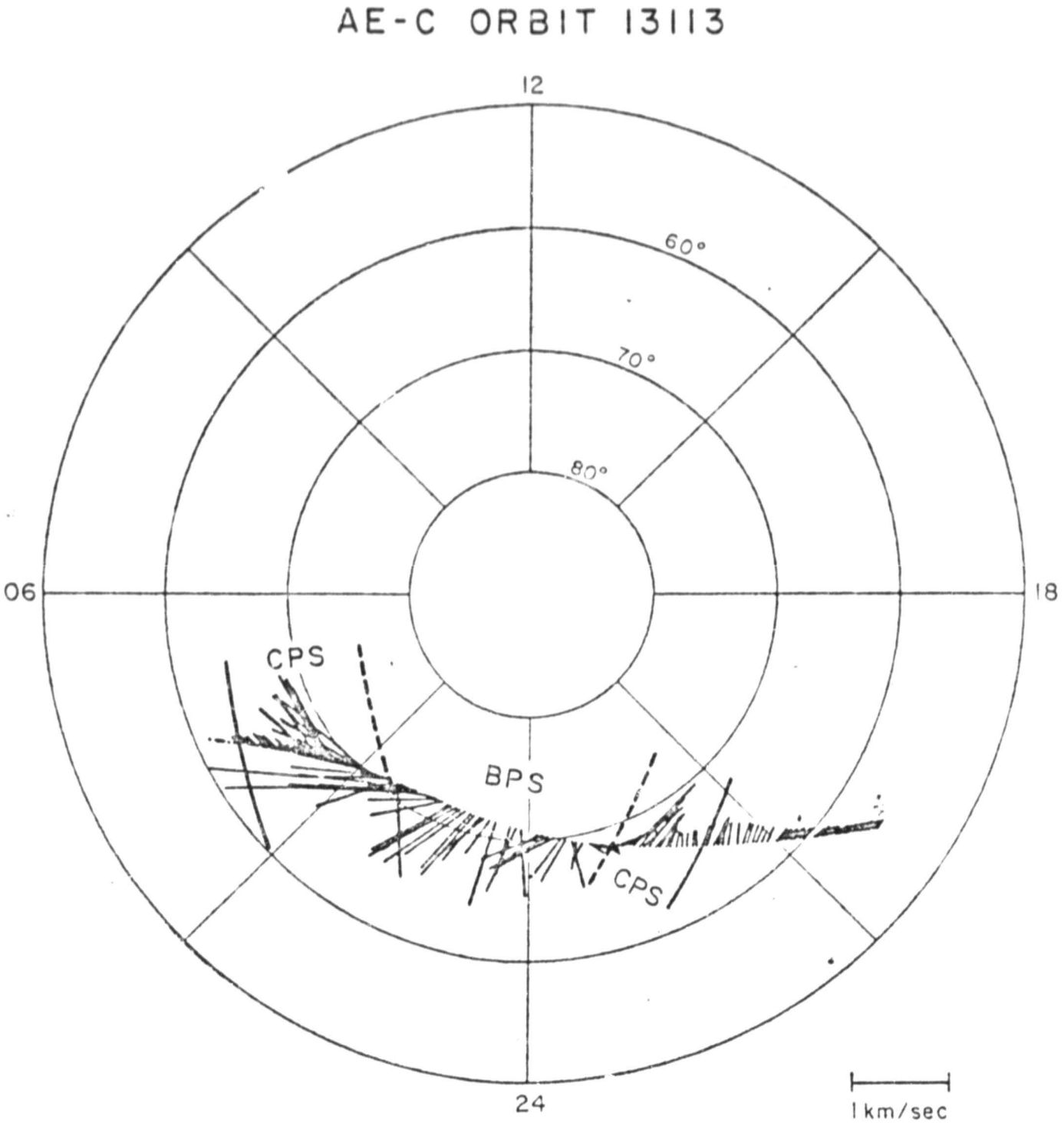

SOUTHERN HEMISPHERE
MLT vs INV LAT

FIGURE 5

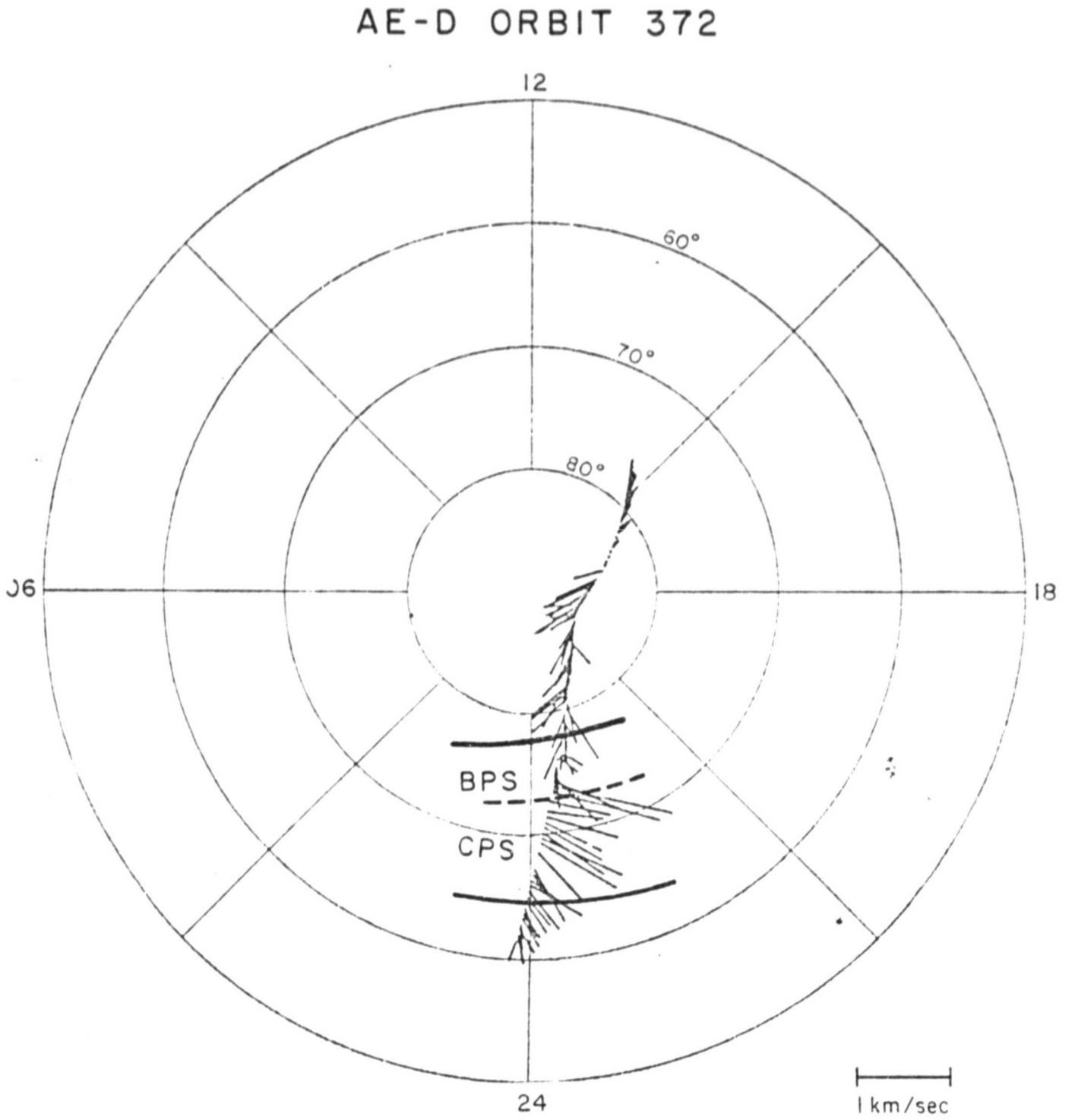
AE-D ORBIT 372
12
60°
70°
80°
06
18
24
BPS
CPS
1 km/sec
NORTHERN HEMISPHERE
MLT vs INV LAT

FIGURE 6

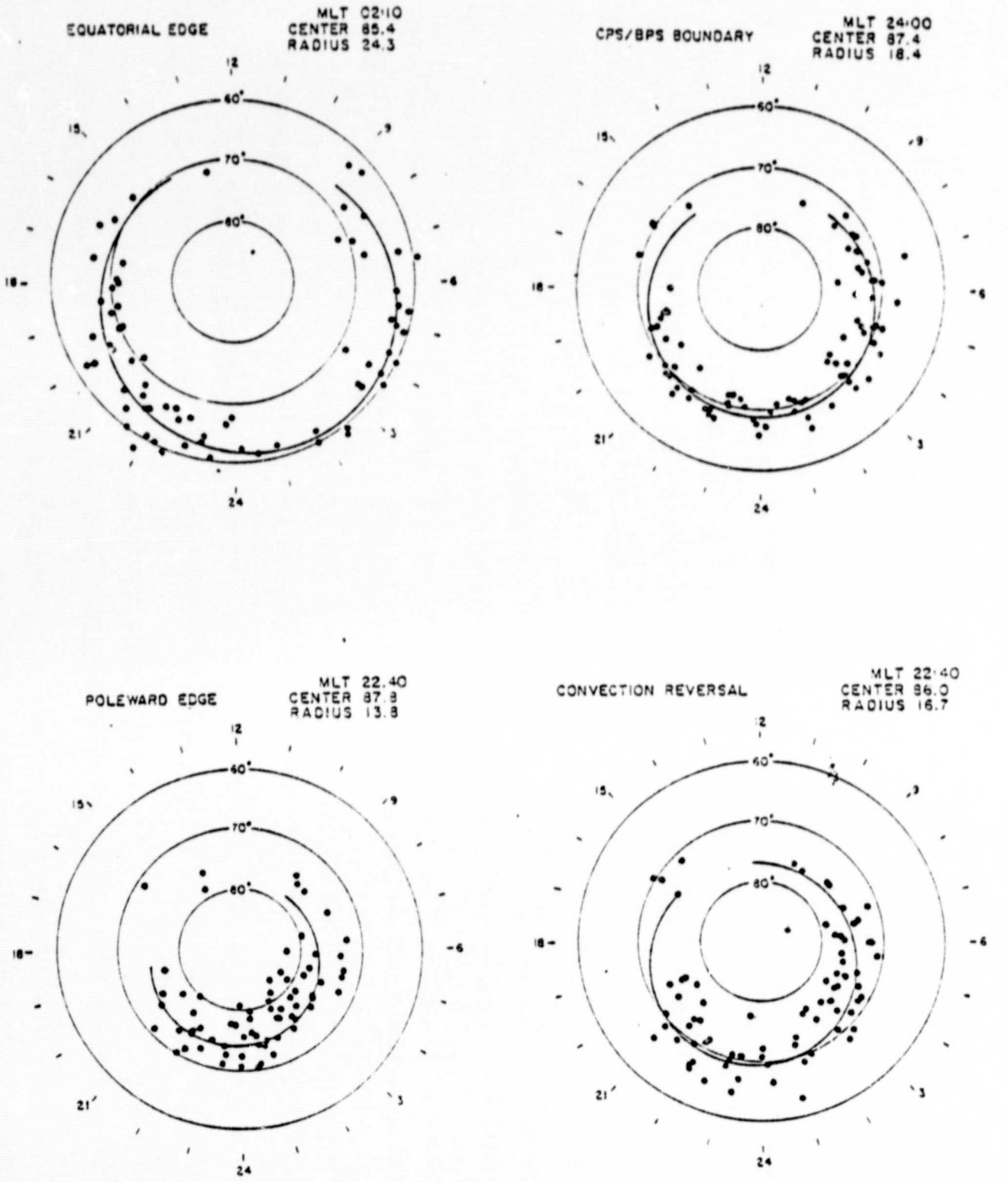
EQUATORIAL EDGE
MLT 02:10
CENTER 65.4
RADIUS 24.3
CPS/BPS BOUNDARY
MLT 24:00
CENTER 87.4
RADIUS 18.4
POLEWARD EDGE
MLT 22.40
CENTER 87.8
RADIUS 13.8
CONVECTION REVERSAL
MLT 22:40
CENTER 86.0
RADIUS 16.7
12
15
9
18
6
21
3
24
60°
70°
80°

FIGURE 7

ORIGINAL PAGE IS
OF POOR QUALITY

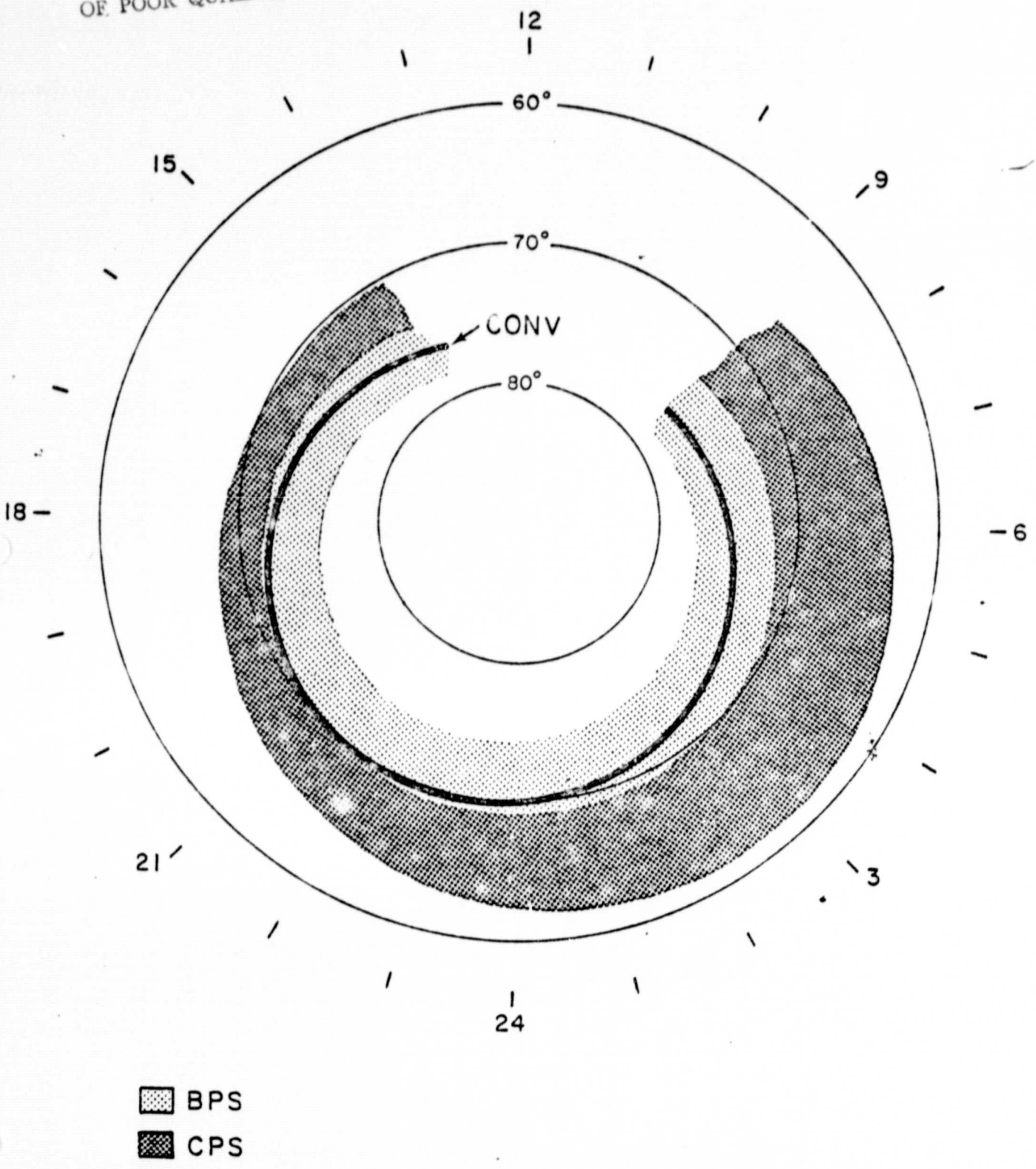

FIGURE 8

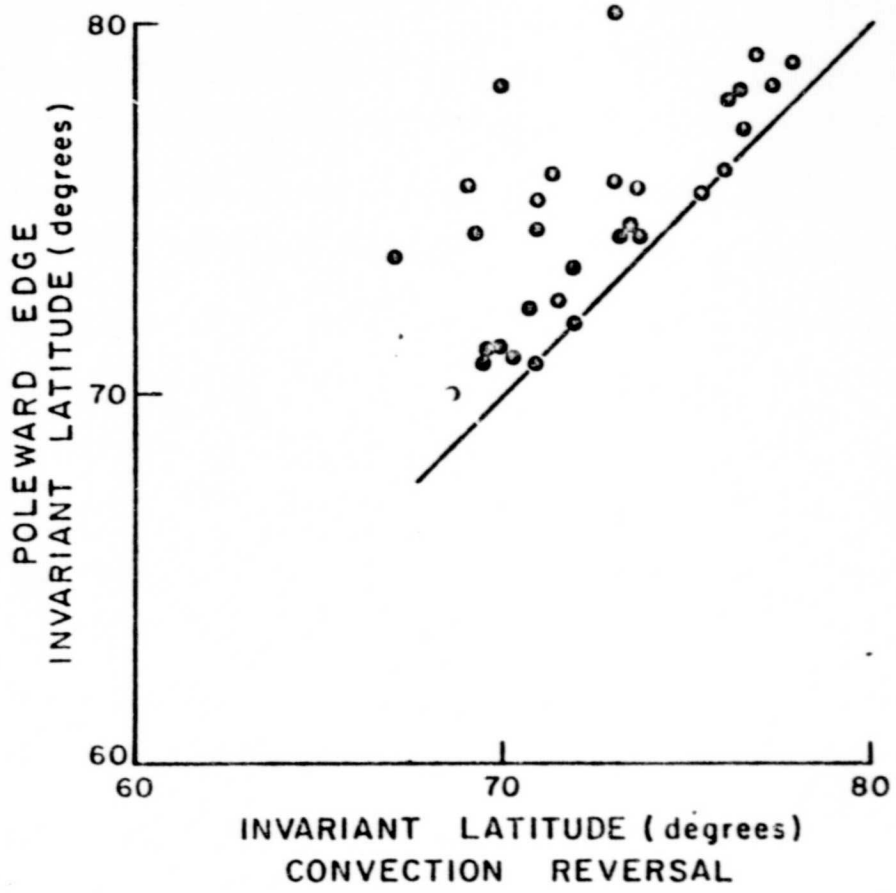

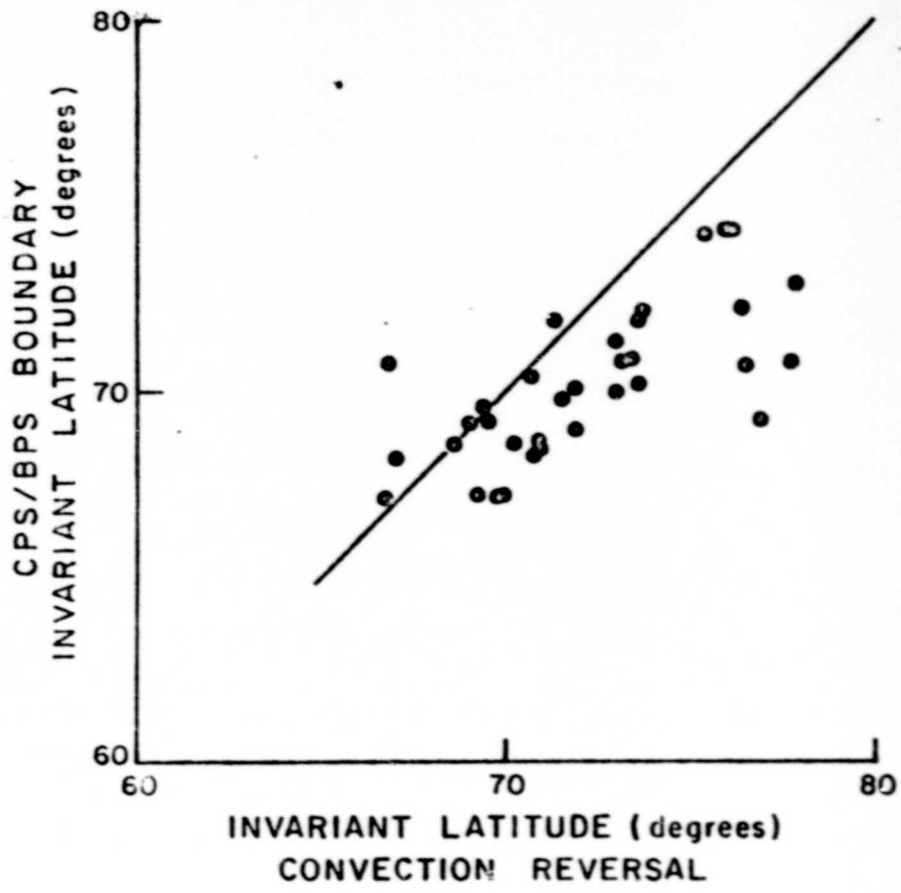

18 - 06 only

FIGURE 9

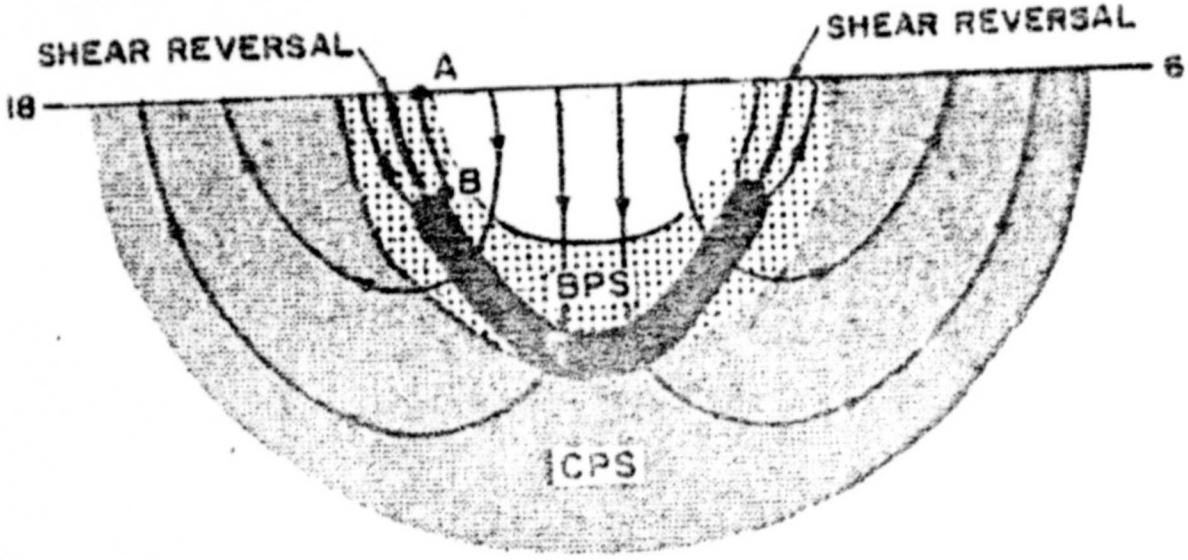

ROTATIONAL REVERSALS

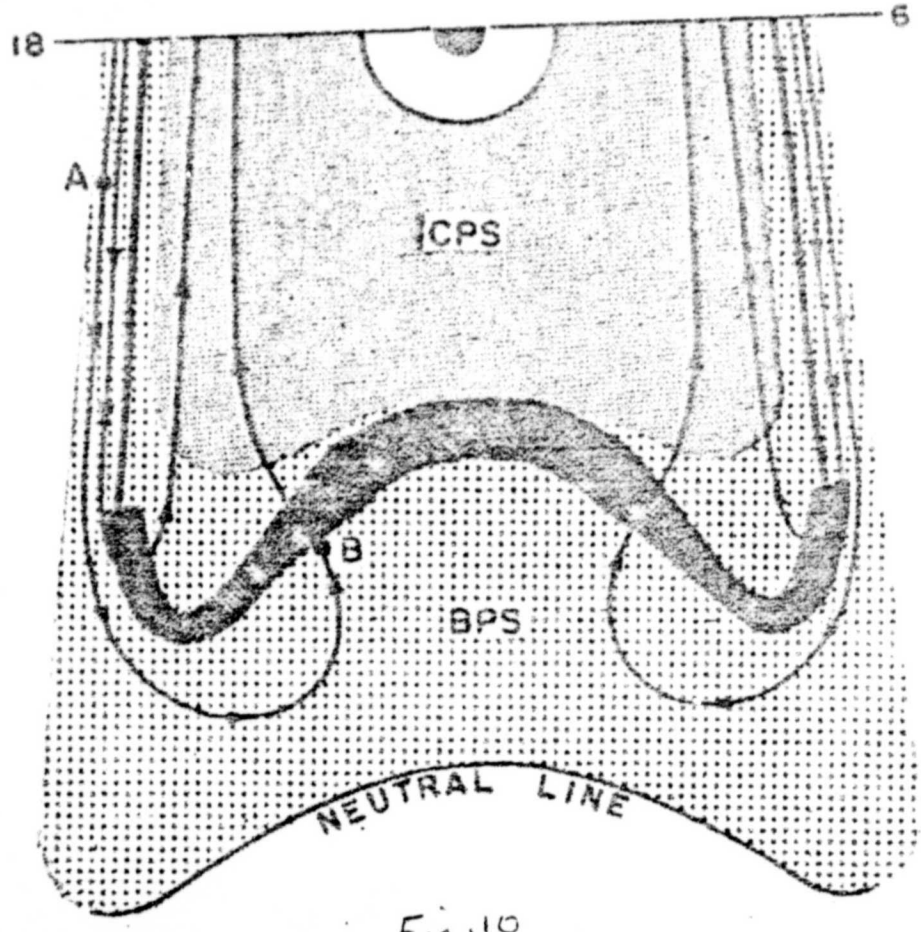

ORIGINAL PAGE
OF POOR QUALITY

Fig. 10